Effect of Pressure on the Proton-Transfer Rate from a Photoacid to a Solvent. 2. 2-Naphthol-6-sulfonate in Water

Pavel Leiderman, Liat Genosar, Nahum Koifman, and Dan Huppert*

Raymond and Beverly Sackler Faculty of Exact Sciences, School of Chemistry, Tel Aviv University, Tel Aviv 69978, Israel

Received: September 30, 2003

The reversible proton dissociation and geminate recombination of the photoacid 2-naphthol-6-sulfonate is studied as a function of pressure in liquid water. Our time-resolved experimental data are analyzed by the reversible diffusion-influenced chemical reaction model. The proton-transfer rate increases significantly with pressure. At 10 kbar the rate increases by about a factor of 8. The main pressure effect is the decrease of the distance between the proton donor and acceptor. The pressure dependence is explained using an approximate stepwise two-coordinate proton-transfer model. The increase in rate as a function of pressure manifests the strong dependence of proton tunneling on the distance between the two heavy atoms which decreases with an increase of pressure.

Introduction

Pressure is known to influence both chemical equilibrium and the rate of chemical reactions in the condensed phase.[1−6] External pressure changes such properties of the medium and reactants as reaction free volume, potential energy profile along the reaction path, compressibility, viscosity, and the reorganization energy of the medium.[7] The absolute value of the reaction rate constant and its temperature dependence can depend on all these parameters.

The phenomenon of excited-state proton transfer (ESPT) from a photoacid molecule, which dissociates upon excitation to produce an excited anion and a proton,[8−11] was used in time-resolved studies of proton-transfer reactions in liquids and solids. Recent studies[12−19] emphasize the dual role played by the solvent molecule as (1) a proton acceptor and (2) a solvating medium of both the reactant and the product.[20−22]

Theoretical studies have revealed that tunneling is the dominant reaction mode for proton transfer, even at ambient temperatures. The theory of proton-transfer reaction in solution was developed by Dogonadze, Kuznetzov, and German[23,24] and then extended by Borgis, Hynes, and Lee,[25] Cukier and Morillo,[26] Voth and co-workers,[27] and Hammes-Schiffer.[28] These theories show that the presence of a potential energy barrier in the proton reaction coordinate causes tunneling through the barrier in the reaction pathway, as opposed to passage over the barrier.

Ando and Hynes[21] studied the acid ionization of HCl in water via a combination of electronic structure calculations and Monte Carlo computer simulations. The mechanism is found to involve the following: first, an activationless (or nearly so) motion in a solvent coordinate, which is adiabatically followed by the quantum proton, to produce a "contact" ion pair Cl^- H_3O^+, which is stabilized by ∼7 kcal/mol; second, motion in the solvent with a small activation barrier, as a second adiabatic proton transfer produces a "solvent-separated" ion pair from the "contact" ion pair in a nearly thermoneutral process.[29]

In recent papers[14−19] we described our experimental results of an unusual temperature dependence of the excited-state proton transfer from a photoacid to liquid water, monols, diols, and glycerol. In methanol and ethanol at temperatures above 285 K the rate of the proton transfer is almost temperature independent, whereas at $T < 250$ K the rate exhibits great temperature dependence. The rate constant is similar to the inverse of the longest component of the dielectric relaxation time of a particular protic solvent. We proposed a simple stepwise model to describe and calculate the temperature dependence of the proton transfer to the solvent reaction. The model accounts for the large difference in the temperature dependence and the proton-transfer rate at high and low temperatures and the solvent dependencies.

The unusual temperature dependence is explained using proton-transfer theory, based on the Landau−Zener curve-crossing formulation. The high-temperature behavior of the rate constant reflects the nonadiabatic limit, whereas the low-temperature behavior denotes the adiabatic limit. We used an approximate expression for the proton-transfer rate, which bridges the nonadiabatic and solvent-controlled adiabatic limit to fit the temperature dependence curve of the experimental proton-transfer rate constant.

Time-resolved fluorescence studies of the photoacid 8-hydroxy-1,3,6-pyrene trisulfonate (HPTS) in water as a function of pressure have been carried out at pressures up to the ice transition point of H_2O.[30] The proton-transfer rates derived from these studies exhibit an increase with pressure from 8×10^9 s^{-1} at 1 atm and 294 K to 2.5×10^{10} s^{-1} at the liquid−ice VI transition point at 9 kbar and 294 K.

In part I we measured,[31] using time-resolved emission techniques, the proton dissociation from a strong photoacid, 5,8-dicyano-2-naphthol (DCN2), and the reversible geminate recombination processes as a function of pressure in ethanol. The experimental time-resolved fluorescence data were analyzed by the exact numerical solution of the transient Debye−Smoluchowski equation (DSE). We found that the proton dissociation rate constant, k_{PT}, of excited DCN2 in neat ethanol at relatively low pressures (up to 10 kbar) increases slightly with pressure,

* Corresponding author: Fax/phone: 972-3-6407012. E-mail: huppert@tulip.tau.ac.il.

10.1021/jp031123j CCC: $27.50
Published on Web 03/06/2004

whereas at higher pressures, up to the freezing point of ethanol, about 1.9 GPa, the proton-transfer rate decreases with pressure, and its value in the high-pressure regime is similar to the inverse of the dielectric relaxation time. The stepwise two-coordinate model that was used to qualitatively fit the temperature dependence was also used to fit the pressure dependence of the proton-transfer rate. In an ethanol solution this analysis of the experimental data showed that the pressure affects both steps but in the opposite direction. The tunneling rate increases with pressure, whereas the solvent relaxation decreases with pressure.

In this paper we further explore the effect of pressure on excited-state intermolecular proton-transfer (ESPT) dynamics. For this purpose we chose a relatively mild photoacid, 2-naphthol-6-sulfonate, pK^* = 1.7 in water.[32] The main finding of this study is that the proton-transfer rate increases appreciably as a function of pressure. Although in previous studies[30,31] the rate increase was relatively small, in this study the rate increases almost 10-fold at the relatively low pressure of 10 kbar (the phase transition point of water−ice VI). We used our qualitative stepwise two-coordinate model to explain the strong pressure effect on proton transfer. The model can be related to theories of proton transfer,[23,25] based on the Landau−Zener curve-crossing formulation.

Experimental Section

Pressurized time-resolved emission was measured in a compact gasketed diamond anvil cell[33] (DAC) purchased from D'Anvil[34,35] with 0.3 carat low fluorescent, high UV transmission diamonds.

To provide a larger volume of the sample for sufficient fluorescent intensity, a 0.45 mm hole was drilled in the 0.8 mm thick stainless gasket. The low fluorescence-type diamonds served as anvils. The anvil seats were equipped with suitable circular apertures for the entry and exit of the exciting laser beam and the excited fluorescent intensity. With this cell pressures up to 30 kbar were reached without detriment to the diamond anvils. The pressure generated was calibrated using the well-known ruby fluorescent technique.[36]

Time-resolved fluorescence was measured using the time-correlated single-photon-counting (TCSPC) technique. As an excitation source we used a CW mode-locked Nd:YAG-pumped dye laser (Coherent Nd:YAG Antares and a 702 dye laser), providing a high repetition rate (>1 MHz) of short pulses (2 ps full width at half-maximum, fwhm). The TCSPC detection system is based on a Hamamatsu 3809U, a photomultiplier, a Tennelec 864 TAC, a Tennelec 454 discriminator, and a personal computer-based multichannel analyzer (nucleus PCA-II). The overall instrumental response was about 50 ps (fwhm). Measurements were taken at 10 nm spectral width. Steady-state fluorescence spectra were taken using a SLM AMINCO-Bowman-2 spectrofluorometer.

2-Naphthol-6-sulfonate was purchased from Kodak and used without further purification. The sample concentrations were between 1×10^{-3} and 3×10^{-4} M, and the sample solutions were made using deionized water of 10 MΩ resistance. The solution's pH was approximately 6.

The fluorescence spectrum belonging to 2-naphthol-6-sulfonate consists of two structureless broad bands (~40 nm fwhm). The emission band maximum of the acidic form (ROH*) in water and alcohols emits at 350 nm. The emission band maximum of the alkaline form (RO^-*) in water and alcohols emits at 420 nm. At 350 nm, the overlap of the two luminescence bands is rather small and the contribution of the RO^-* band to the total intensity at 350 nm is less than 1%. At 1 atm the impurity and dimer emission level is about 0.2% of the peak intensity at 350 nm and increases up to 1% at 10 kbar. Therefore, in the time-resolved analysis, we add to the calculated signal an additional component with an exponential decay of about 10 ns, with an amplitude of about 0.2% at 1 atm, which increases with pressure up to 1% at 10 kbar to account for the impurity fluorescence. To avoid ambiguity from the overlap between the fluorescence contributions of ROH* and RO^-* and in order to minimize the impurity fluorescence, we mainly monitored the ROH* fluorescence at 350 and 450 nm.

SCHEME 1

$$\mathrm{ROH}^* \underset{k_r}{\overset{k_{PT}}{\rightleftharpoons}} [\mathrm{RO}^{-}{}^* \ldots \mathrm{H}^+]_{(r=a)} \overset{\mathrm{DSE}}{\rightleftharpoons} \mathrm{RO}^{-}{}^* + \mathrm{H}^+$$

Results

Reversible Diffusion-Influenced Two-Step Model. Previous studies of reversible ESPT processes in solution led to the development of a reversible diffusion-influenced two-step model[37,38] (Scheme 1).

In the continuous diffusion approach, the photoacid dissociation reaction is described by the spherically symmetric diffusion equation (DSE)[39] in three dimensions.[37,38] The boundary conditions at $r = a$ are those of the back reaction,[38] (Scheme 1). k_{PT} and k_r are the "intrinsic" dissociation and recombination rate constants at the contact sphere radius, a. Quantitative agreement was obtained between the model and the experiment.[37,38] A detailed description of the model, as well as the fitting procedure, is given in refs 14, 37, and 38.

The comparison of the numerical solution with the experimental results involves several parameters. Usually, the adjustable parameters are the proton-transfer rate to the solvent, k_{PT}, and the geminate recombination rate, k_r. The contact radius, a, has acceptable literature values.[37,38] The proton dissociation rate constant, k_{PT}, is determined from the exponential decay at early times of the fluorescence decay. At longer times the fluorescence decay is nonexponential because of the reversible geminate recombination.

An important parameter in our model that strongly influences the nonexponential decay is the mutual diffusion coefficient, $D = D_{H^+} + D_{RO^-}$. The pressure dependence of the proton diffusion constant, D_{H^+}, for water as a function of pressure was measured by Nakahara and Osugi[40] and Franck et al.[41] The proton conductivity slightly increases with pressure. The anion diffusion constant, D_{RO^-}, as a function of pressure was estimated from the water viscosity dependence on pressure data.[42] Figure 1 shows the viscosity dependence on pressure of water at 303 K taken from ref 42. At 20 °C the viscosity slightly decreases at low pressures. At high pressures (>2 kbar), the viscosity slightly increases. At higher temperatures, the viscosity increases with pressure. For comparison, we also display the viscosity dependence on pressure in ethanol.[42,43] Ethanol exhibits a much stronger pressure dependence of the viscosity. Another important parameter in the model is the Coulomb potential between the anion RO^-* and the geminate proton.

$$V(r) = -\frac{R_D}{r}; \quad R_D = \frac{|z_1 z_2| e^2}{\epsilon k_B T} \tag{1}$$

R_D is the Debye radius, z_1 and z_2 are the charges of the proton and anion, ϵ is the static dielectric constant of the solvent, T is the absolute temperature, e is the electronic charge, and k_B is

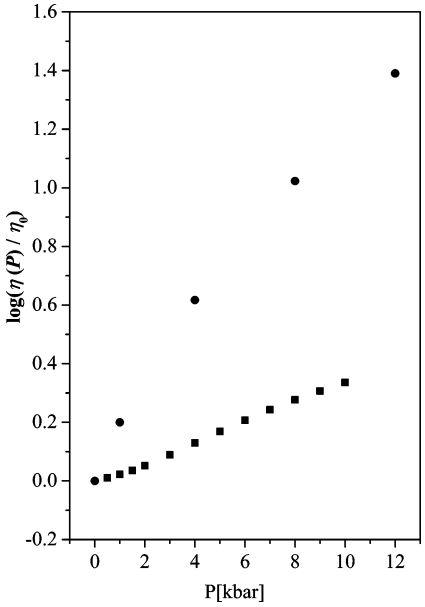

Figure 1. Viscosity dependence on pressure of water and ethanol at 303 K taken from Reference 42. Circles, ●, are ethanol data and squares, ■, are water data.

Boltzmann's constant. The dielectric constant of water[44] and other protic polar liquids increases with pressure.[42]

The asymptotic expression (the long time behavior) for the concentration of ROH* at time t, $[ROH^*]_t$, is given by[45]

$$[ROH^*]_t \cong \frac{\pi}{2} a^2 \exp(R_D/a) \frac{k_r}{k_{PT}(\pi D)^{3/2}} t^{-3/2} \qquad (2)$$

Equation 2 shows that uncertainty in the determination of $D(P)$ causes a larger uncertainty in k_r. Also, the fluorescence "background", due to a fluorescent impurity, and the band overlap prevents us from accurately determining the recombination rate constant. We estimate that the error in the determination of k_{PT} is 10%. The error in the determination of k_{PT} is due to (1) the signal-to-noise ratio of the experimental signal, which affects the quality of the fluorescence signal over longer times and (2) the interplay between k_{PT} and k_r (see eq 2) over longer times. The uncertainty in the determination of k_r is estimated to be much larger, ∼50%. The relatively large uncertainty in the values of k_r arises from the relation between k_r, $D(P)$, and $\epsilon(P)$. In this paper we focus our attention on the pressure dependence of the proton dissociation rate constant, $k_{PT}(P)$, which is measured quite accurately.

Figure 2 shows, on a semilog scale, the experimental time-resolved emission intensity data of 2-naphthol-6-sulfonate in water, measured at 350 nm at various pressures in the range of 0.001−8.6 kbar. To solve the DSE, we used a user-friendly graphic program, SSDP (version 2.61) of Krissinel and Agmon.[46] The experimental data are shown by symbols and the computer fit by solid lines. We determined the proton-transfer rate constant, k_{PT}, from the fit to the initial decay of the ROH* fluorescence (∼800 ps for 2-naphthol-6-sulfonate in water at 1 atm, T = 298 K). The initial decay is mainly determined by the deprotonation process and is almost insensitive to the geminate recombination process. The long time behavior (the fluorescence tail) seen in the ROH* time-resolved emission is a consequence of the repopulation of the ROH* species by the reversible recombination of RO^-* with the geminate proton. The reprotonation of the excited ROH* can undergo a second cycle of deprotonation. The overall effect is

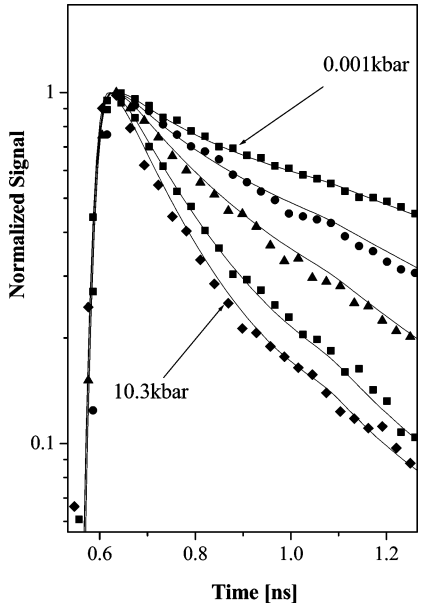

Figure 2. Experimental time-resolved emission intensity data (symbols) at room temperature of 2-naphthol-6-sulfonate in water solution measured at 350 nm at various pressures in the range of 0.001−10 kbar along with the computer fit (solid lines). Squares, ■, 0.001 kbar, circles, ●, 3.1 kbar, triangles, ▲, 5.4 kbar, squares, ■, 8.6 kbar, diamonds, ◆, 10.3 kbar.

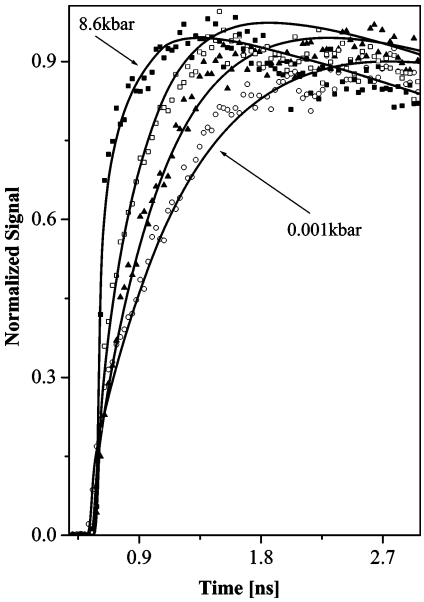

Figure 3. Time-resolved emission at room temperature of 2-naphthol-6-sulfonate RO^-* species in water solution measured at 450 nm at four pressures in the range of 0.001 and 10 kbar. Open circles, ○, 0.001 kbar, filled triangles, ▲ 3.1 kbar, open squares, □, 5.4 kbar, and filled squares, ■, 8.6 kbar.

a nonexponential fluorescence tail.[37] As seen in the figure, over the pressure range of 0.001−10 kbar the decay rate of the fluorescence increases as the pressure increases. The proton-transfer rate constant, k_{PT}, increases with pressure.

Figure 3 shows the time-resolved emission of the 2-naphthol-6-sulfonate RO^-* species in water measured at 450 nm at four pressures in the range of 0.001−8.6 kbar along with the computer fit (solid line) using the reversible proton-transfer model. The parameters used in the fit of the RO^-* luminescence are extracted from the fit of the fluorescence decay curves of ROH* species, measured at 350 nm. The emission intensity at 450 nm has a growth time, which corresponds to the proton-

TABLE 1: Pressure Dependence of the Kinetic Parameters for the Proton-Transfer Reaction of 2-Naphthol-6-sulfonate in Water[a]

P [GPa][b,c]	k_{PT} [10^9 s^{-1}][d]	k_r [10^9 Å s^{-1}][d,e]	D [10^{-5} cm^2 s^{-1}][f]
0.0001	0.9	2.5	9.2
0.13	1.55	5.0	7.0
0.36	2.55	12.0	6.5
0.45	3.55	12.0	5.5
0.85	6.3	13.0	4.5
1.03	7.3	15.0	4.0

[a] For all pressures $1/\tau_{ROH} = 0.12$ ns^{-1}, $1/\tau_{RO^-} = 0.1$ ns^{-1}. [b] 1 GPa $\sim$ 10 kbar. [c] The error in determination of the pressure is $\pm$0.075 Gpa. [d] k_{PT} and k_r are obtained from the fit of the experimental data by the reversible proton-transfer model (see text). [e] The error in the determination of k_r is 50%, see text. [f] Values at high pressures were obtained by best fit to the fluorescence decay.

transfer rate from the 2-naphthol-6-sulfonate ROH* species to water. Figure 3 clearly shows the growth time decrease as the pressure increases (faster rise-time of the fluorescence signal with pressure increase). The radiative decay times of the excited-state RO^-* are only slightly dependent on the pressure. The proton-transfer rate constants, k_{PT} and k_r, at various pressures and the relevant fitting parameters used in the SSDP program to fit the time-resolved emission curves are given in Table 1.

Discussion

In the following section, we first present the basic theoretical concepts related to nonadiabatic and adiabatic proton transfers. This is followed by a description of our stepwise two-coordinate proton-transfer model accounting for both the temperature and pressure dependence of the proton-transfer rate. Finally, we fit the experimental results with our model for proton transfer.

The theory for nonadiabatic proton transfer is very similar to the theory for nonadiabatic electron transfer in its treatment of the involvement of the solvent. In the model,[23] when the polar solvent is equilibrated to the reactant the proton will not be transferred because of an energy mismatch in the reactant and product states. Upon solvent fluctuation, the energy of the reactant and product states becomes equal, and it is in this solvent configuration that the proton tunnels from one side of the well to the other. Finally, upon solvent relaxation, the product state is formed.

If the pretunneling and post-tunneling configurations are regarded as real, transient intermediates, the process can be described by a set of three consecutive chemical equations[47] as shown in Scheme 2, where AH is the protonated photoacid, S_B is a single solvent molecule to which the proton is transferred, S_R is the solvent configuration to stabilize the reactants, and S_p is the solvent configuration of the products. $S^{\neq}$ is the solvent configuration necessary to equally stabilize AH$\cdot\cdot\cdot$$S_B$ and $A^-\cdot\cdot\cdot HS_B^+$. The first equation describes the motion of the solvent configuration to reach the activated solvent configuration. The second equation describes the tunneling process in the proton coordinate. This process only occurs when the energy of the reactant and product states becomes equal. The third equation describes the solvent configuration relaxation toward the bottom of the product well.

One important difference between electron transfer and proton transfer is the extreme sensitivity of the proton-tunneling matrix element to distance. The functional form of the tunneling coupling matrix element, $C(Q_H)$, between the reactant and product state, for moderate to weak coupling, is

$$C(Q_H) = C_0 \exp(-\alpha \delta Q_H) \qquad (3)$$

SCHEME 2

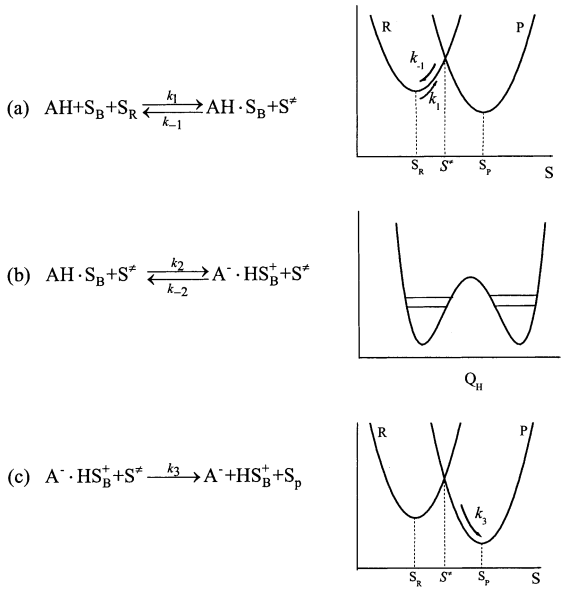

The decay parameter, α, is very large,[25] 25$-$35 Å^{-1}, in comparison with the corresponding decay parameter for the electronic coupling in electron transfer, 1 Å^{-1}. Q_H is the proton coordinate, C_0 is the value of C at the equilibrium position at low pressure, δQ_H is either the change in the intermolecular distance with pressure or the distance change between the two heavy atoms resulting from an intermolecular vibration. It is this feature that makes the dynamics of proton transfer so sensitive to the internuclear separation of the two heavy atoms, and hence, pressure can be used to gradually change the intermolecular distance. For many liquids pressure is known to change the liquid and solid density. The volume decreases by about 25% at about 10 kbar; therefore, the intermolecular distance changes with pressure.

Water at high pressure and temperature between 25 and 85 °C is still "water-like" in its structure. Its hydrogen bond system is hardly affected by these pressures, and its dielectric constant remains high. At high pressures, it support ionization to H_3O^+ and OH^- ions.[48] Wu and Whalley[49] studied the neutron diffraction pattern of liquid D_2O at pressures up to 9.1 kbar at 25 °C.The main conclusions of the diffraction work can be summarized as follows:

(1) Increasing pressure greatly increases the correlation of molecular positions and orientations.

(2) The first-neighbor distances decrease with increasing pressure slower than further neighbor distances, and the compression of water is mostly due to the bending of O$\cdots$O$\cdots$O bonds.

As a first-order approximation the change in intermolecular distance, δQ_H, is related to the change in volume ΔV as $\sqrt[3]{\Delta V}$.

Qualitative Model for the Temperature and Pressure Dependencies of Excited-State Proton-Transfer Reactions. Previously we used a qualitative model that accounts for both the temperature[14$-$17] and, recently,[31] pressure dependencies of the excited-state intermolecular proton transfer to the solvent. We shall use the same model to explain the large pressure dependence of the proton-transfer rate from 2-naphthol-6-sulfonate to water. The proton-transfer reaction depends on two coordinates, the first of which depends on a generalized solvent configuration. The solvent coordinate characteristic time is within the range of the dielectric relaxation time, τ_D, and the longitudinal relaxation, $\tau_L = (\epsilon_0/\epsilon_s)\tau_D$. The second coordinate

is the actual proton translational motion (tunneling) along the reaction path.

The model restricts the proton-transfer process to a stepwise one. The proton moves to the adjacent hydrogen-bonded solvent molecule only when the solvent configuration brings the system to the crossing point. In the stepwise model the overall proton-transfer time is the sum of two times, $\tau = \tau_S + \tau_H$, where τ_S is the characteristic time for the solvent reorganization and τ_H is the time for the proton to pass to the acceptor. The overall temperature and pressure dependent rate constant, $k_{PT}(T, P)$, at a given T and P is

$$k_{PT}(T, P) = \frac{k_H(T, P)k_S(T, P)}{k_H(T, P) + k_S(T, P)} \tag{4}$$

where $k_S(T, P)$ is the solvent coordinate rate constant and $k_H(T, P)$ is the proton coordinate rate constant.

Equation 4 provides the overall excited-state proton-transfer rate constant along the lines of a stepwise process. As a solvent coordinate rate constant, we use

$$k_S(T, P) = b\frac{1}{\tau_D(T, P)} \exp\left(-\frac{\Delta G^{\ddagger}}{RT}\right) \tag{5}$$

where b is an adjustable empirical factor determined from the computer fit of the experimental data. We find that the empirical factor for monols lies between 2 and 4, whereas for water it is larger and lies in the range of 4−8. For the monols τ_L is usually smaller than τ_D by a factor of 2−6 and for water by about a factor of 10. Thus, the solvent characteristic time, $\tau_S = 1/k_S(T,P)$, for water and monols lies between the dielectric relaxation and the longitudinal times, $\tau_L < \tau_S < \tau_D$. The pressure dependence of the dielectric relaxation time up to about ∼1 kbar was measured by Pottel and Asselborn.[50] The dielectric relaxation only slightly increases with pressure over this limited range. It is about 15% slower at 1 kbar than at atmospheric pressure. We are not aware of literature-published values for the dielectric relaxation times as a function of pressure for water at higher pressures up to the freezing pressure of ∼10 kbar.

In many cases the viscosity and τ_D have similar dependencies on both pressure and temperature. As seen in Figure 1, the viscosity dependence on the pressure of water at 30 °C is very mild whereas in ethanol the dependence is much larger. The dielectric relaxation time is often directly proportional to the shear viscosity. This is a direct consequence of the assumed viscous-damped rotating sphere model of dielectric relaxation originally introduced by Debye.[39] In general, the viscosity dependence on pressure is larger than that of the dielectric relaxation. Johari and Dannhauser studied the pressure dependence of the dielectric relaxation of isomeric octanols[51] as well as the pressure dependence of viscosity in isomeric octanols.[52] They found that both the logarithm of viscosity and the logarithm of the dielectric relaxation have, approximately, a linear dependence on pressure, but the slope of the viscosity is slightly larger than that of the dielectric relaxation rate. Figure 4 shows, on a semilogarithm plot, both the viscosity, $\eta(P)$, and the dielectric relaxation time, $\tau_D(P)$, of 2-octanol as a function of pressure. As seen, both viscosity and τ_D have, approximately, a logarithmic dependence on pressure. The viscosity for a particular solvent and temperature has a stronger dependence on the pressure than $\tau_D(P)$.

We used an approximate relation between $\tau_D(P)$ and $\eta(P)$ based on the correspondence between dielectric relaxation and

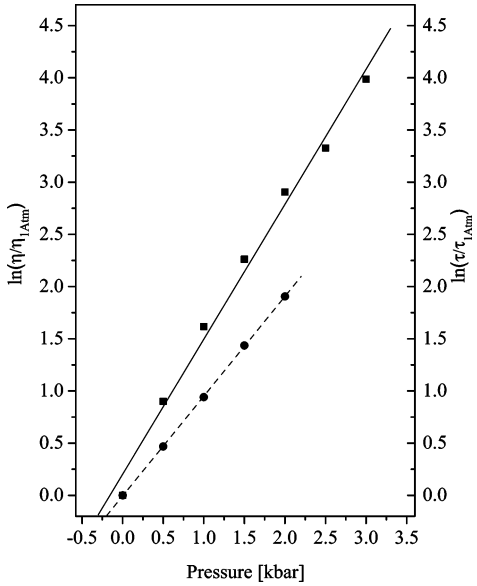

Figure 4. Normalized viscosity $\eta(P)/\eta(1\text{ atm})$ (■) and logarithmic fit (solid line) and the normalized dielectric relaxation time, $\tau_D(P)/\tau_D(1\text{ atm})$ (●) and logarithmic fit (dashed line) as a function of pressure of 2-octanol at 263 K. Data taken from refs 51 and 52.

$\eta(P)$ (see appendix A) to estimate the pressure dependence of the $\tau_D(P)$ of water.

$$\tau_D(P) \sim \tau_D^{1atm}\left(\frac{\eta(P)}{\eta^{1atm}}\right) \exp(-P/P^*) \tag{6}$$

For the best fit to the pressure dependence of k_{PT} using our stepwise model, we used $P^* = 4500$ bar.

The activation energy, $\Delta G^{\ddagger}$, is determined by the Marcus relation

$$\Delta G^{\ddagger} = \frac{1}{4E_S}(E_S + \Delta G)^2 \tag{7}$$

where E_s is the solvent reorganization energy and ΔG is the free energy of the reaction. Thus, one needs to know the excited-state acid equilibrium constant, K_a^* and the solvent reorganization energy. An alternative expression for $\Delta G^{\ddagger}$ can be evaluated from the structure reactivity relation of Agmon and Levine.[53] In our treatment we assume that $\Delta G^{\ddagger}$ is independent of the hydrostatic pressure, and hence, the pressure solely affects the preexponential factor. In a previous study on the temperature dependence of the proton-transfer rate from photoacids to water,[19] we found the activation energies for 2-naphthol (pK^* = 2.7) and 2-naphthol-6,8-disulfonate to be $\Delta G^{\ddagger} = 10$ kJ/mol and 2.5 kJ/mol, respectively. These values agree qualitatively with the Marcus expression for the activation energy (see eq 7). The pK^* value of 2-naphthol-6-sulfonate is between the two compounds mentioned above, p$K^* = 1.7$. We therefore estimate the activation energy value to be $\Delta G^{\ddagger} \approx 3.5$ kJ/mol. The reaction rate constant, k_H, along the proton coordinate, Q_H, is expressed by the usual activated chemical reaction description given by eq 8

$$k_H(P) = k_H^0 \exp\left(-\frac{\Delta G^{\ddagger}}{RT}\right) \tag{8}$$

where k_H^0 is the preexponential factor and $\Delta G^{\ddagger}$ is the activation energy. At high temperatures and/or a high solvent relaxation rate (which is the case for water, $\tau_D = 8$ ps), the actual proton

transfer along the proton-tunneling coordinate, Q_H, is the slower process and hence the rate determining step. This rate strongly depends on pressure because tunneling in the intermediate-coupling case depends exponentially on the intermolecular distance between the two heavy atoms. In this study the proton transfer occurs between the hydroxyl group of 2-naphthol-6-sulfonate and the adjacent oxygen of a hydrogen-bonded water molecule.

As we showed in previous studies,[14−18] $k_H(P)$ is related to the nonadiabatic limit rate expression. In the nonadiabatic limit, the preexponential factor is related to the tunneling coupling matrix element (see eq 3). The coupling matrix element depends strongly on the pressure and increases as the pressure increases.

The effect of pressure and temperature on the photoinduced hydrogen transfer reaction in a mixed crystal of acridine in fluorene was studied by Bromberg et al.[54] The room temperature hydrogen transfer rate increases exponentially when pressure increases. On the basis of proton-tunneling concepts,[55] Trakhtenberg and Klochikhin[7] derived an expression for the pressure and temperature dependence of the tunneling rate of proton transfer in the solid state

$$k(P, T) = \nu \exp[-J(R_0) + J'R_0(1 - \alpha_P^{-1/3}) + J'^2\delta_{CN}^{\ 2}/8\alpha_P^{\ \gamma} \coth(\hbar\Omega_0\alpha_P^{\ \gamma}/4k_BT)] \quad (9)$$

where $\alpha_P(P) = V_0/V(P)$, Ω_0 is the effective frequency of the intermolecular vibration, δ_{CN}^2 is the square of the amplitude of the intercenter C···N distance, and $\gamma = -\partial\ln\Omega_0/\partial\ln V$.

$$J(R) = (2/\hbar)\int\{2m[U(x, R) - E_H(R)]\}^{1/2}\,dx \quad (10)$$

$E_H(R)$ and $U(x, R)$ are the total and potential energies of the tunneling atom, respectively, depending on the distance, R, between the two heavy atoms (in our case two oxygen atoms). R_0 is the equilibrium distance between the heavy atoms and J' is the derivative, $\partial J/\partial R$. The first term on the right-hand side of eq 9 is the usual tunneling expression and does not account for the pressure effect. The second term accounts for the change with pressure of the equilibrium position between the two heavy atoms. The third term takes into account the pressure effect on the intermolecular low frequency. Trakhtenberg and Klochikhin[7] found good correspondence with the experimental results of Bromberg et al.[54] when they used a smaller power dependence of the compressibility, α_P (0.22 instead of $^1/_3$ as expected from the relation of distance and volume).

In our previous pressure study of DCN2 in ethanol, we estimated the pressure dependence of the proton coordinate rate constant, $k_H(P)$, from the second term of eq 9 with a compressibility dependence on power of 0.22. In the current work we used the value of 0.33 because for the first approximation $\delta Q_H = \sqrt[3]{\Delta V}$. For $\Omega_0 = 5.0 \times 10^{13}\ s^{-1}$, $\delta_{O-O}^2 = 0.005\ Å^2$, $\gamma = 2.2$ (the values are taken from ref 7), we find that the third term in eq 9 decreases the tunneling rate as the pressure increases. The rate decreases by about 30% at about 10 kbar. At higher pressures the value of the third term is about the same as at 10 kbar because the volume compressibility is very small at high pressures. In our treatment we neglected the contribution to the pressure dependence of the third term in eq 9. Thus, the change in the proton-tunneling rate constant as a function of pressure is given by

$$\frac{k_H(P)}{k_H(1\ \text{atm})} \cong \exp[J'R_0(1 - \alpha_P^{-0.33})] \quad (11)$$

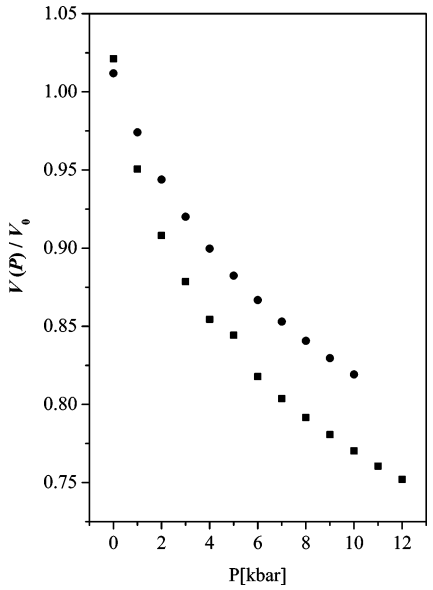

Figure 5. Pressure dependence of $1/\alpha_P = V_P/V_0$ of water and ethanol. Squares, ■, are ethanol data and circles, ●, are water data.

Figure 5 shows the dependence of $1/\alpha_P = V_P/V_0$ on pressure, for water, and for comparison, we also added the pressure dependence of $1/\alpha_P$ for ethanol, where V_P for both liquids are taken from ref 42. In water, alcohols, and many other liquids, the change in volume with pressure over a pressure range of up to 10 kbar is very similar. The compressibility, $1/V\ (\partial V/\partial P)_T$, decreases with pressure increase. In general, it is smaller for water than for methanol and ethanol. For water and ethanol it changes by a factor of about 3 and 5 between atmospheric pressure and 10 kbar, respectively.

Figure 6 shows a fit to the stepwise two-coordinate model of $k_{PT}(P) = k_H(P)k_S(P)/(k_H(P) + k_S(P))$ as a function of pressure (solid line) along with the experimental data (dots). The results of 2-naphthol-6-sulfonate in water show a large increase of the proton-transfer rate with pressure changes. At about 10 kbar the rate is about 10-fold larger than the rate at atmospheric pressure. We show the pressure dependence of the proton-tunneling rate constant, using eq 11, and the following parameters: $J' = 14.2\ Å^{-1}$, $R_0 = 2.4$ Å, $J'R_0 = 34$; α_P was taken from ref 42. As seen, the rate increases as a function of pressure. The tunneling rate constant, in our model k_H, increases with pressure, from atmospheric pressure to 10 kbar, by a factor of 8. The value of the solvent-controlled adiabatic rate constant, k_S at atmospheric pressure is larger by about 2 orders of magnitude than k_H. Whereas k_H increases 10-fold with pressure, k_S decreases with pressure by only a factor of 2. Because $k_S \gg k_H$ at all pressures, the value of the overall rate constant (eq 4), k_{PT}, is determined mainly by the slowest rate constant, that is, k_H. The total rate $k_{PT}(T, P)$ increases with pressure by a factor of 8 at about 1 GPa, the water−ice VI transition point. Because $1/\alpha_P$ is not constant with pressure, but rather decreases as the pressure increases, $k_H(P)/k_H(1\ \text{atm})$ does not increase with the same initial slope. In Figure 6b we also show, for comparison, the pressure dependence of DCN2 in ethanol taken from our previous study.[31] The results of DCN2 in ethanol show an initial increase of the rate with the pressure. At about 8 kbar the rate reaches a maximum value, $k_{PT}(8\ \text{kbar}) = 2k_{PT}(1\ \text{atm})$. Further increase of the pressure decreases the rate constant of the proton transfer to the solvent. This interesting observation of the pressure dependence of the proton-transfer rate from DCN2 to ethanol is explained by the opposite pressure dependencies of k_H and k_S and the saturation of k_H at medium-pressure values.

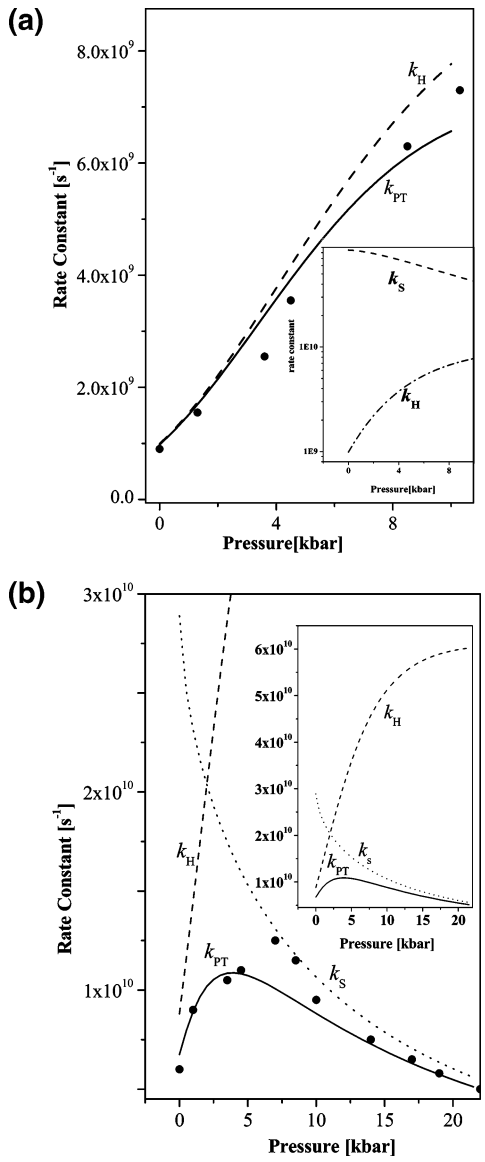

Figure 6. Fit to the stepwise two-coordinate model of $k_{PT}(P) = k_H(P)k_S(P)/(k_H(P) + k_S(P))$ as a function of pressure (solid line) along with the experimental data (dots). $k_H(P)$ and $k_S(P)$ are shown as dashed and dotted lines, respectively. The inset shows the calculated rate constants. (a) 2-Naphthol-6-sulfonate in water. (b) DCN2 in ethanol.

The pressure dependence of k_{PT}, k_H, and k_S for 2-naphthol-6-sulfonate in water and DCN2 in ethanol are also plotted (dotted lines) in parts a and b of Figure 6, respectively.

Summary

We studied, using time-resolved emission techniques, the proton dissociation and reversible geminate recombination from the photoacid 2-naphthol-6-sulfonate to water as a function of pressure. The experimental time-resolved fluorescence data are analyzed by the exact numerical solution of the transient Debye−Smoluchowski equation (DSE).[46]

We found that the proton dissociation rate constant, k_{PT}, of excited 2-naphthol-6-sulfonate in water up to the pressure of the freezing point (~10 kbar), increases by about a factor of 8 with pressure. We compared these results with our previous pressure work on DCN2 in ethanol.

We used a stepwise two-coordinate model to qualitatively fit the pressure dependence of the proton-transfer rate. We previously used this model to explain the temperature dependence of the proton-transfer rate from various photoacids to solvents.[15−19] Recently,[31] we also employed the model to account for the pressure dependence of the proton-transfer rate from DCN2 to ethanol as a function of pressure. The analysis of the experimental data by the model shows that the pressure affects both steps but in opposite directions. In the case of proton transfer from 2-naphthol-6-sulfonate to water, pressure only mildly affects the solvent coordinate rate, k_S. In contrast to k_S, the tunneling rate, k_H, increases almost 10-fold with pressure. The overall effect is the strong increase of the rate with pressure.

Acknowledgment. We thank Professor M. Pasternak and Dr. G. Rozenberg for providing the diamond anvil cell high-pressure technology. This work was supported by Grants from the US−Israel Binational Science Foundation and the James−Franck German−Israel Program in Laser−Matter Interaction.

Appendix A

Johari and Dannhauser studied the pressure dependence on both the viscosity and the relaxation times[52] of isomeric octanols over a range of temperatures and pressures up to 4 kbar. The results of the viscosity pressure dependence of a certain octanol isomer at a particular temperature can be approximated by

$$\ln\frac{\eta_P}{\eta_0} = aP \tag{A1}$$

where η_P and η_0 are the viscosity values at pressure P and at atmospheric pressure, respectively and a is the slope of the linear dependence on pressure of the logarithm of the viscosity. The slope a depends on the temperature and the specific octanol isomer. A similar expression can be found for the pressure dependence of the dielectric relaxation

$$\ln\frac{\tau_D(P)}{\tau_D^0} = a'P \tag{A2}$$

which leads to $\tau_D(P) = \tau_D^0 \exp(a'P)$. It was found, experimentally, that for a certain octanol at a specific temperature $a > a'$, that is, the pressure dependence of the viscosity is larger than that of the dielectric relaxation. Using eqs A1 and A2 and rearranging the expression, we obtain eq A3:

$$\tau_D(P) = \tau_D^0\left(\frac{\eta_P}{\eta_0}\right)\exp((a' - a)P) \tag{A3}$$

If we denote $a' - a = -1/P^*$, we get eq 6 in the text. From this relation we can use the literature data of the viscosity pressure dependence of a certain liquid and hence deduce the pressure dependence of the liquid dielectric relaxation time, $\tau_D(P)$.

References and Notes

(1) Asano, T.; le Noble, W. J. *Chem. Rev.* **1978**, *78*, 407.
(2) Kelm, H., Ed.; High-Pressure Chemistry; Reidel: Dordrecht, The Netherlands, 1978.
(3) Le Noble, W. J.; Kelm, H. *Angew. Chem., Int. Ed. Engl.* **1980**.
(4) Van Eldik, R.; Asano, T.; le Noble, W. *J. Chem. Rev.* **1989**, *89*, 549.
(5) Rollinson, A. M.; Drickamer, H. G. *J. Chem. Phys.* **1980**, *73*, 5981.
(6) Schroeder, J. *J. Phys.: Condens. Matter* **1996**, *8*, 9379.
(7) Trakhtenberg, L. I.; Klochikhin, V. L. *Chem. Phys.* **1998**, *232*, 175.
(8) Ireland, J. F.; Wyatt, P. A. H. *Adv. Phys. Org. Chem.* **1976**, *12*, 131.
(9) (a) Huppert, D.; Gutman, M.; Kaufmann, K. J. In *Advances in Chemical Physics*; Jortner, J., Levine, R. D., Rice, S. A., Eds.; Vol. 47; Wiley: New York, 1981; p 681. (b) Kosower, E. M.; Huppert, D. In *Annual*

Reviews of Physical Chemistry; Strauss, H. L., Babcok, G. T., Moore, C. B., Eds.; Vol. 37; Annual Reviews Inc.: Palo Alto, CA, 1986; p 122.
(10) Lee, J.; Robinson, G. W.; Webb, S. P.; Philips, L. A.; Clark, J. H. *J. Am. Chem. Soc.* **1986**, *108*, 6538.
(11) Gutman, M.; Nachliel, E. *Biochim. Biophys. Acta* **1990**, *391*, 1015.
(12) Knochenmuss, R. *Chem. Phys. Lett.* **1998**, *293*, 191.
(13) Peters, S.; Cashin, A.; Timbers, P. *J. Am. Chem. Soc.* **2000**, *122*, 107.
(14) Poles, E.; Cohen, B.; Huppert, D. *Isr. J. Chem*. **1999**, *39*, 347.
(15) Cohen, B.; Huppert, D. *J. Phys. Chem. A* **2000**, *104*, 2663.
(16) Cohen, B.; Huppert, D. *J. Phys. Chem. A* **2001**, *105*, 2980.
(17) Cohen, B.; Huppert, D. *J. Phys. Chem. A*, **2002**, *106*, 1946−1955.
(18) Cohen, B.; Segal, J.; Huppert, D., *J. Phys. Chem. A* **2002**, *106*, 7462−7467.
(19) Cohen, B.; Leiderman, P.; Huppert, D. *J. Phys. Chem. A* **2002**, *106*, 11115−11122.
(20) Kolodney, E.; Huppert, D. *J. Chem. Phys.* **1981**, *63*, 401.
(21) Ando, K.; Hynes, J. T. In *Structure, Energetics and Reactivity in Aqueous Solution*; Cramer, C. J., Truhlar, D. G., Eds.; American Chemical Society: Washington, DC, 1994.
(22) Agmon, N.; Huppert, D.; Masad, A.; Pines, E. *J. Phys. Chem.* **1991**, *96*, 952.
(23) German, E. D.; Kuznetsov, A. M.; Dogonadze, R. R. *J. Chem. Soc., Faraday Trans. 2* **1980**, *76*, 1128.
(24) Kuznetsov, A. M. *Charge Transfer in Physics, Chemistry and Biology*; Gordon and Breach: Amsterdam, 1995.
(25) (a) Borgis, D.; Hynes, J. T. *J. Phys. Chem.* **1996**, *100*, 1118. (b) Borgis, D. C.; Lee, S.; Hynes, J. T. *Chem. Phys. Lett.* **1989**, *162*, 19. (c) Borgis, D.; Hynes, J. T. *J. Chem. Phys.* **1991**, *94*, 3619.
(26) (a) Cukier, R. I.; Morillo, M. *J. Chem. Phys.* **1989**, *91*, 857. (b) Morillo, M.; Cukier, R. I. *J. Chem. Phys.* **1990**, *92*, 4833.
(27) (a) Li, D.; Voth, G. A. *J. Phys. Chem.* **1991**, *9*, 10425. (b) Lobaugh, J.; Voth, G. A. *J. Chem. Phys.* **1994**, *100*, 3039.
(28) Hammes-Schiffer, S. *Acc. Chem. Res*. **2001**, *34*, 273−281.
(29) Ando, K.; Hynes J. T. *J. Phys. Chem. B* **1997**, *101*, 10464.
(30) Huppert, D.; Jayaraman, A.; Maines, R. G., Sr.; Steyert, D. W.; Rentzepis, P. M. *J. Chem. Phys.* **1984**, *81*, 5596.
(31) Koifman, N., Cohen, B.; Huppert, D. *J. Phys. Chem A*. **2002**, *106*, 4336−4344.
(32) Weller, A. *Prog. React. Kinet.* **1961**, *1*, 189.
(33) Jayaraman, A. *Rev. Mod. Phys.* **1983**, *55*, 65.
(34) Machavariani, G. Yu.; Pasternak, M. P.; Hearne, G. R.; Rozenberg, G. K. *Rev. Sci. Instrum.* **1998**, *69*, 1423.
(35) D'ANVILS is administered by Ramot Ltd., 32 H. Levanon Str., Tel Aviv 61392, Israel. http://www.tau.ac.il/ramot/danvils.
(36) Barnett, J. D.; Block, S.; Piermarini, G. J. *Rev. Sci. Instum.* **1973**, *44*, 1.
(37) Pines, E.; Huppert, D.; Agmon, N. *J. Chem. Phys.* **1988**, *88*, 5620.
(38) Agmon, N.; Pines, E.; Huppert, D. *J. Chem. Phys.* **1988**, *88*, 5631.
(39) Debye, P. *Trans. Electrochem. Soc.* **1942**, *82*, 265.
(40) Nakahara, M.; Osugi, J. *Rev. Phys. Chem. Jpn* **1980**, *50*, 66.
(41) Franck, E. U.; Hartmann, D.; Hensel, F. *Discuss. Faraday Soc*. **1965**, *39*, 200.
(42) Bridgman, P. E. *The Physics of High Pressure;* G. Bell and Sons Ltd.: London, 1958.
(43) *Landolt-Bornstein*; Andrussow, L., Schramm, B., Eds.;Vol. 2, Part 5a; Springer: Berlin, 1969.
(44) (a) Heger, K.; Uematsu, M.; Franck, E. U. *Ber. Bunsenges. Phys. Chem.* **1980**, *84*, 758. (b) Srinvasan, K. R.; Kay, R. L. *J. Chem. Phys.* **1974**, *60*, 3645.
(45) Agmon, N.; Goldberg, S. Y.; Huppert, D. *J. Mol. Liq.* **1995**, *64*, 161.
(46) Krissinel, E. B.; Agmon, N. *J. Comput. Chem*. **1996**, *17*, 1085.
(47) (a) Kreevoy, M. M.; Kotchevar, A. T. *J. Am. Chem. Soc.* **1990**, *112*, 3579. (b) Kotchevar, A. T.; Kreevoy, M. M. *J. Phys. Chem.* **1991**, *95*, 10345.
(48) Hamann, S. D. *High-Pressure Physics and Chemistry*; Bradley, R. S., Ed.; Academic Press: New York, 1963; pp 131−162.
(49) Wu, A. Y.; Whalley, E. *J. Mol. Phys*. **1982**, *47*, 603.
(50) Pottel, R.; Asselborn, E. *Ber. Bunsen-Ges. Phys. Chem*. **1980**, *84*, 462.
(51) Johari, G.; Dannhauser, W. *J. Chem. Phys.* **1969**, *50*, 1862.
(52) Johari, G.; Dannhauser, W. *J. Chem. Phys.* **1969**, *51*, 1626.
(53) (a) Agmon, N.; Levine, R. D. *Chem. Phys. Lett.* **1977**, *52*, 197. (b) Agmon, N.; Levine, R. D. *Isr. J. Chem.* **1980**, *19*, 330.
(54) Bromberg, S.; Chan, I.; Schilke, D.; Stehlik, D. *J. Chem. Phys.* **1993**, *98*, 6284.
(55) Goldanskii, V. I.; Trakhtenberg, L. I.; Fleuorov, V. N. *Tunneling Phenomena in Chemical Physics*: Gordon and Breach: New York, 1989; Chapter IV.